



## EXPERIMENTAL AND ANALYTICAL INVESTIGATION OF A FLUTTERING BRIDGE SECTION MODEL

Zsolt Szabó and Gábor Stépán

*Department of Applied Mechanics, Budapest University of Technology and Economics (BME),  
Budapest, Hungary 1521,  
e-mail: szabo.zs@mm.bme.hu*

Ambrus Zelei

*HAS-BUTE Research Group on Dynamics of Machines and Vehicles, Budapest, Hungary 1111*

Flutter instability is a typical aerodynamic vibration phenomenon of slender elastic bridges. The sensitivity for flutter can be predicted by determining the so-called flutter derivatives from the small-scale model of the bridge. This work investigates an elastic supported two d.o.f. bridge section model which can move vertically and rotate around a horizontal axis. These movements correspond to the bending and torsional vibrations of the bridge. The linearised equations of motion is assumed to be known, thus, the aerodynamic forces can be determined from wind-tunnel experiments. These forces are assumed as linear functions of the generalised coordinates and their time-derivatives. The coefficients of the linear terms called also as flutter derivatives depend on the flow (wind) velocity. These coefficients are to be determined by the Monte Carlo method using the measured acceleration data. The obtained results are compared to the results determined by curve-fitting on the acceleration time-signal. The original (structural) damping and stiffness matrices can be modified by using the flutter derivatives since the equations of motion form a homogeneous linear differential equation system. Thus, we get effective damping and stiffness matrices. Flutter instability occurs when a harmonic solution satisfies the equations. The critical flow velocity which the system loses its stability at is also compared to the stability boundary of the analytical model based on Theodorsen's approach.

---

### 1. Introduction

Slender, flexibly supported structures subjected by aerodynamic effects can lose their stability through vibrations called flutter which is a self-excited vibration.<sup>1</sup> The phenomenon can be investigated on a simplified model, a rigid section of it supported by springs which corresponds to the elasticity of the whole structure. The aerodynamic forces depending on the position and the velocity of the body are quite complicated and there exists analytical expressions in closed forms only for special cases such quasi-steady potential flow or unsteady potential flow with undamped vibration.<sup>2</sup> Therefore, the so-called *flutter derivatives* are to be determined from experiments<sup>3</sup> or numerical simulations.<sup>4,5</sup>

The experiments were carried out in Theodore von Kármán Wind Tunnel Laboratory at the Department of Fluid Mechanics, BUTE. The experimental rig contained a flat rectangular bridge section supported by 8 springs of stiffness  $k$  at its corners. Its width perpendicular to the flow of

density  $\rho$  was  $l$ . The body was assumed to have only two degree-of-freedom (DoF) in the plane of its cross-section parallel to the flow and the lateral motion was negligible.

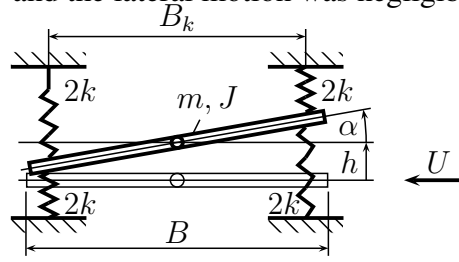


Figure 1: Mechanical model of the bridge section.

The two DoF mechanical model can be seen in Fig. 1. The body of the bridge section was modelled as a rigid bar of length  $B$ , mass  $m$  with centre of gravity in the middle. The mass moment of inertia w.r.t. the centre of gravity is denoted by  $J$ . The supporting springs are located symmetrically in a distance  $B_k$  from each other. The values of the mentioned parameters are listed in Table 1.

Table 1: Parameter values of the bridge section model.

$m = 30 \text{ kg}$	$\rho = 1.25 \text{ kg/m}^3$
$J = 1.31 \text{ kgm}^2$	$k = 908.7 \text{ N/m}$
$B = 0.6 \text{ m}$	$B_k = 0.5 \text{ m}$
$l = 1.62 \text{ m}$	

## 2. Analytical studies

The generalised coordinates representing the two degrees of freedom are the vertical displacement  $h$  of the C.o.G from the equilibrium and the angle  $\alpha$  between the horizontal plane and the plane of the bridge section. That is,  $q_1 = h$  and  $q_2 = \alpha$  and the body is in equilibrium for  $h = \alpha = 0$ .

The equations of motion has the following form:

$$\mathbf{M}\ddot{\mathbf{q}} + \mathbf{C}_{mech}\dot{\mathbf{q}} + \mathbf{K}_{mech}\mathbf{q} = \mathbf{Q}_{flow}, \quad (1)$$

where

$$\mathbf{M} = \begin{bmatrix} m & 0 \\ 0 & J \end{bmatrix}, \quad \mathbf{C}_{mech} = \begin{bmatrix} c_h & 0 \\ 0 & c_\alpha \end{bmatrix}, \quad \mathbf{K}_{mech} = \begin{bmatrix} 8k & 0 \\ 0 & 2B_k^2k \end{bmatrix},$$

and  $\mathbf{Q}_{flow}$  is the generalised force depending on the flow. The elements  $c_h$  and  $c_\alpha$  of the damping matrix  $\mathbf{C}_{mech}$  were determined from measurement data obtained for the case  $U = 0$ .

It can be seen that the vertical and rotational vibrations are decoupled if there is no exciting force. The undamped natural angular frequencies are

$$\omega_1 = \sqrt{\frac{8k}{m}} \quad \text{and} \quad \omega_2 = \sqrt{\frac{2B_k^2k}{J}} \equiv \frac{B_k}{2r_i}\omega_1 \quad \text{with} \quad r_i = \sqrt{\frac{J}{m}}. \quad (2)$$

### 2.1 Quasi-steady potential flow

As it was shown in<sup>6</sup> the generalised force has the form

$$\mathbf{Q}_{flow} = \frac{\rho}{2}lB \cdot 2\pi \begin{bmatrix} -U\dot{h} + U^2\alpha \\ -\frac{B}{4}U\dot{h} + \frac{B}{4}U^2\alpha \end{bmatrix} \quad (3)$$

assuming quasi-steady potential flow of velocity  $U$  and small displacements.

Introducing dimensionless quantities like  $\eta = 4h/B$  and  $\tau = t\omega_1$  we can rewrite Eq. (1) as follows:

$$\mathbf{q}'' + \begin{bmatrix} 2\zeta_1 & 0 \\ 0 & 2\zeta_2\varepsilon \end{bmatrix} \mathbf{q}' + \begin{bmatrix} 1 & 0 \\ 0 & \varepsilon^2 \end{bmatrix} \mathbf{q} = u \begin{bmatrix} -4\mu & 0 \\ -4\vartheta & 0 \end{bmatrix} \mathbf{q}' + u^2 \begin{bmatrix} 0 & 16\mu \\ 0 & 16\vartheta \end{bmatrix} \mathbf{q}, \quad (4)$$

where  $\mathbf{q} = (\eta, \alpha)$ , the prime (') denotes  $d/d\tau$ ,  $u$  is the dimensionless flow velocity and

$$\zeta_1 = \frac{c_h}{2\sqrt{8mk}}, \quad \zeta_2 = \frac{c_\alpha}{2\sqrt{2JB_k^2k}}, \quad \varepsilon = \frac{\omega_2}{\omega_1} \equiv \frac{B_k}{2r_i}, \quad u = \frac{U}{B\omega_1},$$

$$\mu = \frac{\rho l B^2 \pi}{4m}, \quad \vartheta = \frac{\rho l B^4 \pi}{64J} \equiv \mu\beta^2, \quad \beta = \frac{B}{4r_i}.$$

Table 2 concludes the values of the introduced parameters for the investigated model.

Table 2: Derived parameter values.

$r_i$ [m]	$\omega_1$ [rad/s]	$\omega_2$ [rad/s]	$\varepsilon$ [-]	$\mu$ [-]	$\vartheta$ [-]	$\beta$ [-]
0.209	15.6	18.6	1.20	0.0191	0.00983	0.718

Eq. (4) is a linear system and its stability can be investigated according to the Routh–Hurwitz criterion. The characteristic equation contains a fourth order polynomial:

$$\lambda^4 + a_3\lambda^3 + a_2\lambda^2 + a_1\lambda + a_0 = 0 \quad (5)$$

with the coefficients

$$a_3 = 2(\zeta_2\varepsilon + \zeta_1 + \mu u), \quad (6)$$

$$a_2 = 1 + \varepsilon^2 - 16\vartheta u^2 + 4(\zeta_1 + 2\mu u)\zeta_2\varepsilon, \quad (7)$$

$$a_1 = 2(\zeta_2\varepsilon + (\zeta_1 + 2\mu u)\varepsilon^2 - 16\vartheta u^2\zeta_1), \quad (8)$$

$$a_0 = \varepsilon^2 - 16\vartheta u^2. \quad (9)$$

Finally, we obtain that the following two inequalities determine the stability:

$$a_0 > 0 \quad \wedge \quad a_3(a_1a_2 - a_3a_0) - a_1^2 > 0.$$

The first condition yields a critical flow velocity  $u_{cr,0}$  which depends on the ratio of the natural frequencies linearly:

$$u < u_{cr,0} = \frac{\varepsilon}{4\beta\sqrt{\mu}}.$$

At this critical value  $\lambda = 0$  which means static stability loss.

However, the other condition can be solved only numerically and one can show that the critical flow velocity can be smaller than  $u_{cr,0}$  only if  $\varepsilon > 1$ . At this boundary  $\lambda = i\tilde{\omega}$  that is the loss of stability happens via vibrations called as *flutter*.

## 2.2 Unsteady potential flow

Though, the unsteady model is expected to be more accurate than the quasi-steady one, it cannot be solved analytically for arbitrary case. However, the coefficients of the flow forces can be derived assuming harmonic motions (*i.e.* critical case) according to Theodorsen's approach:<sup>2</sup>

$$\mathbf{Q}_{flow} = \frac{\rho l B \pi}{4} U \begin{bmatrix} H_1 & \frac{B}{4} H_2 \\ \frac{B}{4} A_1 & \frac{B}{16} A_2 \end{bmatrix} \dot{\mathbf{q}} + \frac{\rho l \pi}{4} U^2 \begin{bmatrix} H_4 & \frac{B}{4} H_3 \\ \frac{B}{4} A_4 & \frac{B}{16} A_3 \end{bmatrix} \mathbf{q}, \quad (10)$$

where

$$H_1 = A_1 = -4F(k), \quad (11)$$

$$H_2 - 8 = A_2 = 4 \left( -1 + F(k) + \frac{2G(k)}{k} \right), \quad (12)$$

$$H_4 - 4k^2 = A_4 = 8kG(k), \quad (13)$$

$$A_3 - 2k^2 = H_3 = -4A_1 - A_4. \quad (14)$$

The approximation of the functions  $F(k)$  and  $G(k)$  was given by Starossek:<sup>7</sup>

$$F(k) \approx 1 - \frac{0.165k^2}{k^2 + 0.0455^2} - \frac{0.335k^2}{k^2 + 0.09}, \quad (15)$$

$$G(k) \approx -\frac{0.165 \cdot 0.0455k}{k^2 + 0.0455^2} - \frac{0.335 \cdot 0.3k}{k^2 + 0.09}, \quad (16)$$

where  $k = B\omega/2U$ , the dimensionless frequency of oscillation.

Thus, the dimensionless form of the equations of motion is as follows

$$\mathbf{q}'' + \begin{bmatrix} 2\zeta_1 & 0 \\ 0 & 2\zeta_2\varepsilon \end{bmatrix} \mathbf{q}' + \begin{bmatrix} 1 & 0 \\ 0 & \varepsilon^2 \end{bmatrix} \mathbf{q} = u \begin{bmatrix} \mu H_1 & \mu H_2 \\ \vartheta A_1 & \vartheta A_2 \end{bmatrix} \mathbf{q}' + u^2 \begin{bmatrix} \mu H_4 & \mu H_3 \\ \vartheta A_4 & \vartheta A_3 \end{bmatrix} \mathbf{q}, \quad (17)$$

however, this is true only for harmonic solutions. Similarly, only the pure imaginary roots ( $\lambda = i\tilde{\omega}$ ) of the corresponding characteristic polynomial can be accepted.<sup>1</sup> This yields two equations — one for the imaginary part and one for the real part:

$$-a_3(\tilde{\omega}, u)\tilde{\omega}^2 + a_1(\tilde{\omega}, u) = 0, \quad (18)$$

$$\tilde{\omega}^4 - a_2(\tilde{\omega}, u)\tilde{\omega}^2 + a_0(\tilde{\omega}, u) = 0. \quad (19)$$

Fixing all of the parameters but  $u$ ,  $\varepsilon$  and  $\tilde{\omega}$  the stability boundary can be found numerically as a parametric curve  $(\varepsilon(\tilde{\omega}), u_{cr}(\tilde{\omega}))$ .

### 3. Experimental investigations

During the wind-tunnel experiments the acceleration signals were recorded at the four corners of the bridge section for two typical initial conditions and five different flow velocities as listed in Tables 3 and 4.

Table 3: Approximate initial conditions (IC).

	$h(0)$	$\alpha(0)$	$\dot{h}(0)$	$\dot{\alpha}(0)$
<i>disp:</i>	$h_0$	0	0	0
<i>rot:</i>	0	$\alpha_0$	0	0

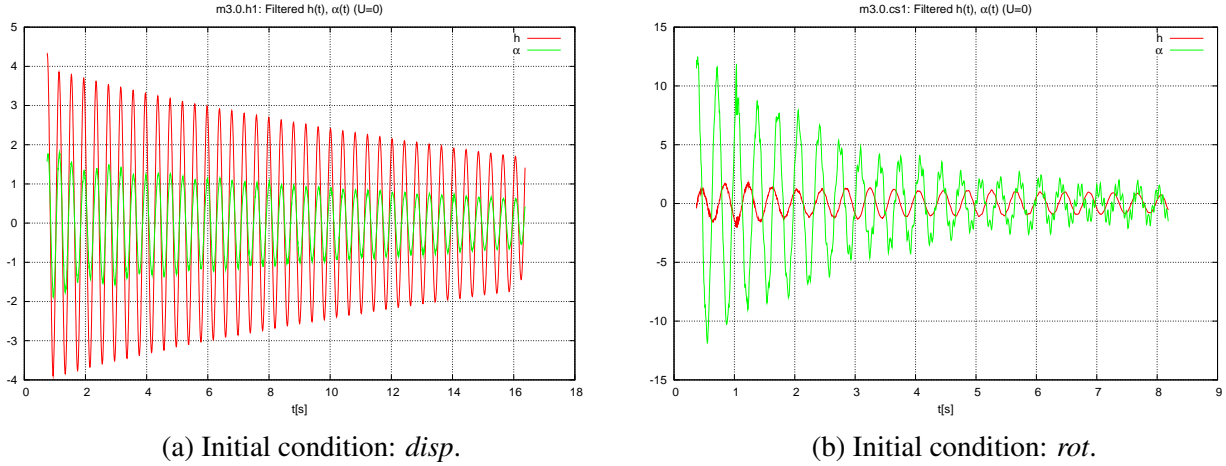
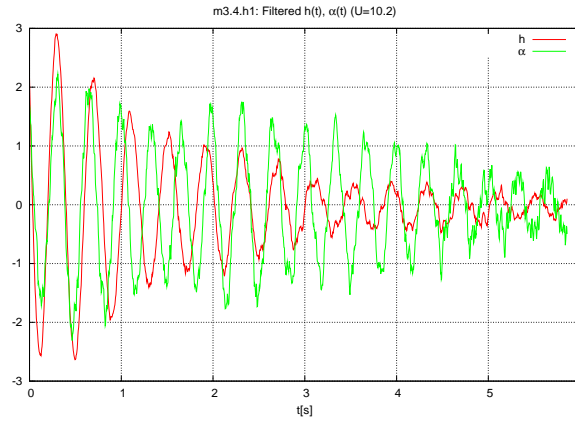
Table 4: Flow velocities.

<i>i:</i>	1	2	3	4	5
$U_i$ [m/s]:	0	1.9	5	7.9	10.2

The values of  $\ddot{h}(t)$  and  $\ddot{\alpha}(t)$  were determined from the four acceleration signals. The values of  $h(t)$  and  $\alpha(t)$  were obtained by filtering and integrating the acceleration values. The time-plots of these filtered data for  $U = 0$  and  $U = 10.2$  m/s can be seen in Figs. 2 and 3.

In the case  $U = 10.2$ , the displacement  $h(t)$  was still damped, however, the angular displacement  $\alpha(t)$  was not which showed near-critical state. That is  $u_{cr} \approx 10.2/.6/15.6 = 1.09$  at  $\varepsilon \approx 1.20$ .

<sup>1</sup>Here,  $\tilde{\omega} = \omega/\omega_1$  is another dimensionless form of the oscillation frequency in the dimensionless time-domain  $\tau$ .


 Figure 2: Time-plots for  $U = 0$ .

 Figure 3: Time-plots for  $U = 10.2$  m/s (initial condition *disp.*).

### 3.1 Least Square Method

Assuming small displacements the effects of the flow forces can be included into the damping and stiffness matrices of the system resulting so-called *effective* damping and stiffness matrices:

$$\mathbf{M}\ddot{\mathbf{q}} + \mathbf{C}_{eff}(U)\dot{\mathbf{q}} + \mathbf{K}_{eff}(U)\mathbf{q} = \mathbf{0}. \quad (20)$$

Both the solution  $\mathbf{q}(t)$  of such linear system and its acceleration  $\ddot{\mathbf{q}}(t)$  have the form:

$$\ddot{\mathbf{q}}(t) = \mathbf{D}\mathbf{E}(t) \equiv \begin{bmatrix} \mathbf{d}_{11} & \mathbf{d}_{12} & \mathbf{d}_{21} & \mathbf{d}_{22} \end{bmatrix} \begin{bmatrix} e^{\beta_1 t} \cos \gamma_1 t \\ e^{\beta_1 t} \sin \gamma_1 t \\ e^{\beta_2 t} \cos \gamma_2 t \\ e^{\beta_2 t} \sin \gamma_2 t \end{bmatrix}. \quad (21)$$

The values of  $\beta_i$  and  $\gamma_i$  can be approximated from the FFT analysis of the signals. These approximations can be later improved using an iterative method. Now, we can determine the elements of matrix  $\mathbf{D}$  using the Least Square Method:

$$\mathbf{R} = \sum_i (\mathbf{D}\mathbf{E}(t_i) - \ddot{\mathbf{q}}(t_i))^2 \equiv (\mathbf{D}\hat{\mathbf{E}} - \hat{\mathbf{Q}})(\mathbf{D}\hat{\mathbf{E}} - \hat{\mathbf{Q}})^T \rightarrow \min! \quad (22)$$

where

$$\hat{\mathbf{Q}} = [q_i(t_j)] \quad \text{and} \quad \hat{\mathbf{E}} = [\mathbf{E}[i](t_j)].$$

Thus, the partial derivatives w.r.t. the elements of  $\mathbf{D}$  yield

$$(\mathbf{D}\hat{\mathbf{E}} - \hat{\mathbf{Q}})\hat{\mathbf{E}}^\top = \mathbf{0} \quad \Rightarrow \quad \mathbf{D} = \hat{\mathbf{Q}}\hat{\mathbf{E}}^\top(\hat{\mathbf{E}}\hat{\mathbf{E}}^\top)^{-1}. \quad (23)$$

At this point we can modify the values of the damped natural angular frequencies  $\gamma_1$  or  $\gamma_2$  (depending on whether it is a *disp* or a *rot* signal) and try to find another matrix  $\mathbf{D}$  for an even smaller residual vector  $\mathbf{R}$ . Table 5 shows the values of the obtained  $\gamma_i$  and  $\beta_i$  and the relative damping calculated from them.

Table 5: Natural frequencies and relative dampings for  $U = 0$ .

$i$	$\gamma_i$	$\beta_i$	$\omega_i = \sqrt{\gamma_i^2 + \beta_i^2}$	$\zeta_i = -\beta_i/\omega_i$
1:	15.6	-0.0526	15.6	.00339
2:	18.6	-0.4170	$18.6 \approx 1.2\omega_1$	.02240

One can easily show that the relation between the displacement, velocity and acceleration is the following:

$$\ddot{\mathbf{q}}(t) = \mathbf{D}\mathbf{E}(t), \quad \dot{\mathbf{q}}(t) = \mathbf{D}\mathbf{J}^{-1}\mathbf{E}(t), \quad \mathbf{q}(t) = \mathbf{D}\mathbf{J}^{-2}\mathbf{E}(t), \quad (24)$$

where

$$\mathbf{J} = \begin{bmatrix} \mathbf{J}_1 & \mathbf{0} \\ \mathbf{0} & \mathbf{J}_2 \end{bmatrix} \quad \text{and} \quad \mathbf{J}_i = \begin{bmatrix} \beta_i & -\gamma_i \\ \gamma_i & \beta_i \end{bmatrix}.$$

Substituting these formulas into Eq. (20) we get:

$$(\mathbf{M}\mathbf{D} + \mathbf{C}_{eff}\mathbf{D}\mathbf{J}^{-1} + \mathbf{K}_{eff}\mathbf{D}\mathbf{J}^{-2})\mathbf{E}(t) = \mathbf{0}. \quad (25)$$

Since the vector  $\mathbf{E}(t)$  can be arbitrary depending on the time, the matrix expression in the parenthesis must be zero. Expressing the system matrices to be found, we obtain:

$$\begin{bmatrix} \mathbf{C}_{eff} & \mathbf{K}_{eff} \end{bmatrix} = -\mathbf{M}\mathbf{D} \begin{bmatrix} \mathbf{D}\mathbf{J}^{-1} \\ \mathbf{D}\mathbf{J}^{-2} \end{bmatrix}^{-1}, \quad (26)$$

and the matrices containing the flutter derivatives:

$$\mathbf{C}_{flow} = \mathbf{C}_{mech} - \mathbf{C}_{eff} \quad \text{and} \quad \mathbf{K}_{flow} = \mathbf{K}_{mech} - \mathbf{K}_{eff}. \quad (27)$$

### 3.2 The Monte Carlo Method

The coefficient matrices of the flow forces given in Eq. (27) can be determined directly from the linear equation of motion if we know the values of  $\mathbf{q}$ ,  $\dot{\mathbf{q}}$  and  $\ddot{\mathbf{q}}$  in four different time instants. The matrices  $\mathbf{M}$ ,  $\mathbf{C}_{mech}$  and  $\mathbf{K}_{mech}$  are also assumed to be known. That is, Eq. (1) at  $t = t_i$  has the form

$$\mathbf{M}\ddot{\mathbf{q}}(t_i) + \mathbf{C}_{mech}\dot{\mathbf{q}}(t_i) + \mathbf{K}_{mech}\mathbf{q}(t_i) = \mathbf{C}_{flow}\dot{\mathbf{q}}(t_i) + \mathbf{K}_{flow}\mathbf{q}(t_i). \quad (28)$$

It can be rewritten in the form of a linear algebraic equation system for the time instants  $t_1, t_2, t_3$  and  $t_4$ :

$$\mathbf{L} \equiv \begin{bmatrix} \mathbf{l}(t_1) & \mathbf{l}(t_2) & \mathbf{l}(t_3) & \mathbf{l}(t_4) \end{bmatrix} = \begin{bmatrix} \mathbf{C}_{flow} & \mathbf{K}_{flow} \end{bmatrix} \mathbf{A}, \quad (29)$$

where

$$\mathbf{l}(t_i) = \mathbf{M}\ddot{\mathbf{q}}(t_i) + \mathbf{C}_{mech}\dot{\mathbf{q}}(t_i) + \mathbf{K}_{mech}\mathbf{q}(t_i), \quad \mathbf{A} = \begin{bmatrix} \dot{\mathbf{q}}(t_1) & \dot{\mathbf{q}}(t_2) & \dot{\mathbf{q}}(t_3) & \dot{\mathbf{q}}(t_4) \\ \mathbf{q}(t_1) & \mathbf{q}(t_2) & \mathbf{q}(t_3) & \mathbf{q}(t_4) \end{bmatrix}. \quad (30)$$

If matrix  $\mathbf{A}$  is regular then matrices  $\mathbf{C}_{flow}$  and  $\mathbf{K}_{flow}$  can be determined. Though, choosing the time instants randomly it can happen that matrix  $\mathbf{A}$  is not invertable or the elements of the matrices determined again and again can be very different. However, doing this procedure a *lot* of time, one can do statistics on the obtained results and take the average and standard deviation of the generated data.

## 4. Results

The critical flow velocity which the system loses its stability at depending on the natural frequency ratio is shown in Fig. 4. The stable domain in the plane of  $\varepsilon$ ,  $u$  is larger for the unsteady model than the domain for the quasi-steady case. The blue star belongs to the experimentally detected critical case which is close to the quasi-steady stability boundary. This seems to question the validity of the unsteady model, however, more experiments are needed to be able to validate the critical points at different natural frequency ratios.

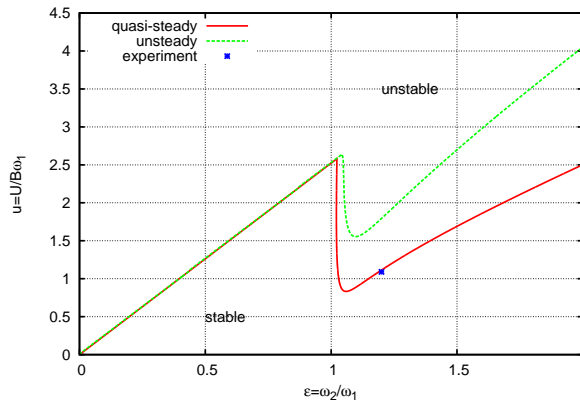


Figure 4: Stability charts of the quasi-steady and unsteady models.

## 5. Conclusions

In this paper the two DoF planar motions of a bridge section was investigated. Assuming a quasi-steady potential flow the equations of motion can be derived for small vibrations and Routh–Hurwitz criterion yields the implicit expressions of the stability boundaries both for the cases of static and dynamic stability loss. Using the model of unsteady potential flow in the case of critical non-decaying vibrations a modified boundary curve was obtained. Experiments were also done at various wind speed and a critical value was detected which the vibrations do not decay above.

A modified experimental rig is needed that makes possible to set up other natural frequency ratios ( $\varepsilon$ ), e.g. by changing the distance  $B_k$  of the supporting springs. Using such modified experimental setup the other points of the stability boundary can be checked, as well.

## Acknowledgements

This research was supported by the Hungarian–Chinese bilateral fund for science and technology under grant number TÉT\_12\_CN-1-2012-0012.

## REFERENCES

- <sup>1</sup> C. Borri and C. Costa. Bridge Aerodynamics and Aeroelastic Phenomena — Chapter 1: Bridges. In Ted Stathopoulos, editor, *Wind Effects on Buildings and Design of Wind-Sensitive Structures*, CISM Courses and Lectures No. 493. Springer Wien New York, 2007.
- <sup>2</sup> T. Theodorsen. General theory of aerodynamic instability and the mechanism of flutter. Technical Report 496, National Advisory Committee for Aeronautics (NACA), 1935.
- <sup>3</sup> Özgür Avşar. Determination of flutter derivatives from free vibration test results. Master’s thesis, Institut für Baustatik und Stahlbau, Technische Universität Hamburg-Harburg, 2003.

- <sup>4</sup> G. Szabó and G. Kristóf. Three-dimensional numerical flutter simulation. In *The 5th International Symposium on Computational Wind Engineering (CWE2010), Chapel Hill, North Carolina, USA, 2010*.
- <sup>5</sup> G. Szabó and J. Györgyi. Numerical simulation of the flutter performance of different generic bridge cross sections. *Periodica Polytechnica, Ser. Civil Eng.*, 55(2):137–146, 2011.
- <sup>6</sup> Zs. Szabó, A. Zelei, and G. Stépán. Stability of an elastic supported flat plate subjected to potential flow. *Periodica Polytechnica, Ser. Mech. Eng.*, 56(2):99–103, 2012.
- <sup>7</sup> U. Starossek. *Brückendynamik — Winderregte Schwingungen von Seilbrücken*. Vieweg, 1992.